Peritoneal Dialysis International, Vol. 33, pp. 132–142
doi: 10.3747/pdi.2011.00234

0896-8608/13 $3.00 + .00

22-OXACALCITRIOL PREVENTS PROGRESSION OF PERITONEAL FIBROSIS IN A MOUSE MODEL

Misaki Hirose,[1] Tomoya Nishino,[1] Yoko Obata,[1,2] Masayuki Nakazawa,[1] Yuka Nakazawa,[1] Akira Furusu,[1] Katsushige Abe,[3] Masanobu Miyazaki,[4] Takehiko Koji,[5] and Shigeru Kohno[1]

Second Department of Internal Medicine,[1] Nagasaki University School of Medicine, Nagasaki; Medical Education Development Center,[2] Nagasaki University Hospital, Nagasaki; Jinnikai Hospital,[3] Oita; Miyazaki Clinic,[4] Nagasaki; and Department of Histology and Cell Biology,[5] Nagasaki University School of Medicine, Nagasaki, Japan

♦ ***Objective:*** **Vitamin D plays an important role in calcium homeostasis and is used to treat secondary hyperparathyroidism among dialysis patients. The biologic activity of vitamin D and its analogs is mediated by vitamin D receptor (VDR), which is distributed widely throughout the body. Recent papers have revealed that low vitamin D levels are correlated with severe fibrosis in chronic diseases, including cystic fibrosis and hepatitis. The aim of the present study was to evaluate the protective effects of vitamin D against the progression of peritoneal fibrosis.**

♦ ***Methods:*** **Peritoneal fibrosis was induced by injection of chlorhexidine gluconate (CG) into the peritoneal cavity of mice every other day for 3 weeks. An analog of vitamin D, 22-oxacalcitriol (OCT), was administered subcutaneously daily from initiation of the CG injections. The peritoneal tissue was excised at 3 weeks. Changes in morphology were assessed by hematoxylin and eosin staining. Expression of VDR, alpha smooth muscle actin (as a marker of myofibroblasts), type III collagen, transforming growth factor β (TGF-β), phosphorylated Smad2/3, F4/80 (as a marker of macrophages), and monocyte chemoattractant protein-1 (MCP-1) was examined by immunohistochemistry. Southwestern histochemistry was used to detect activated nuclear factor κB (NF-κB).**

♦ ***Results:*** **In the CG-injected mice, immunohistochemical analysis revealed expression of VDR in mesothelial cells, myofibroblasts, and macrophages in the thickened submesothelial zone. Treatment with OCT significantly prevented peritoneal fibrosis and reduced the accumulation of type III collagen in CG-treated mice. Among the markers of fibrosis, the numbers of myofibroblasts, cells positive for TGF-β, and cells positive for phosphorylated Smad2/3 were significantly decreased in the OCT-treated group compared with the vehicle-treated group. Furthermore, OCT suppressed inflammatory mediators of fibrosis, as shown by the reduced numbers of activated NF-κB cells, macrophages, and MCP-1–expressing cells.**

♦ ***Conclusions:*** **Our results indicate that OCT attenuates peritoneal fibrosis, an effect accompanied by reduced numbers of myofibroblasts, infiltrating macrophages, and TGF-β–positive cells, suggesting that vitamin D has potential as a novel therapeutic agent for preventing peritoneal sclerosis.**

Perit Dial Int **2013; 33(2):132-142 www.PDIConnect.com**
epub ahead of print: 02 Oct 2012 doi:10.3747/pdi.2011.00234

KEY WORDS: Vitamin D; 22-oxacalcitriol; peritoneal fibrosis; TGF-β; MCP-1; NF-κB; southwestern histochemistry.

Although peritoneal dialysis (PD) is a beneficial treatment for patients with end-stage renal disease, long-term PD causes morphologic (1) and functional changes in the peritoneum. Characteristic pathology findings include marked peritoneal fibrosis and massive accumulation of collagen in the submesothelial area (2,3). In particular, some patients with peritoneal fibrosis develop encapsulating peritoneal sclerosis, which is one of the most critical complications of PD, being associated with high mortality. However, the mechanism of peritoneal fibrosis in PD patients remains poorly understood, and no effective therapy is currently available.

Vitamin D—specifically, its most active metabolite, 1,25-dihydroxyvitamin D_3 (calcitriol)—plays important roles in a variety of biologic processes such as calcium homeostasis, hormone secretion, and cell proliferation and differentiation (4,5). Most pleiotropic actions of vitamin D and its analogs are mediated by the

Correspondence to: T. Nishino, Second Department of Internal Medicine, Nagasaki University School of Medicine, 1-7-1 Sakamoto, Nagasaki 852-8501 Japan.
tnishino@nagasaki-u.ac.jp
Received 15 September 2011; accepted 8 March 2012

specific vitamin D receptor (VDR), a ligand-dependent transcription factor that belongs to the steroid nuclear receptor gene family (6,7). Recent studies have reported a ubiquitous distribution of VDR, including in kidney, bone, parathyroid gland, intestine, skin, lung, pancreas, and heart, and in cells such as lymphocytes, macrophages, and fibroblasts (8–10).

Fibrosis is characterized as overgrowth, hardening, or scarring of various tissues, and it is attributed to excess deposition of extracellular matrix components such as collagen. Early events in fibrosis include differentiation of fibroblasts into myofibroblasts by the action of transforming growth factor β (TGF-β) (11). The differentiated cells in turn act as major producers of collagen. Thus, from a therapeutic viewpoint, interfering with the pathways that lead to an expansion of the myofibroblast population would be a possible approach.

Few studies have investigated the impact of vitamin D on the development of fibrosis. For instance, a previous *in vitro* study reported that vitamin D suppresses the activation of renal interstitial myofibroblasts and therefore collagen expression (9). In a unilateral model of ureteral obstruction, vitamin D suppressed renal interstitial fibrosis, collagen deposition, and myofibroblast expansion detected using the selective cell marker alpha smooth muscle actin (α-SMA) (12). Furthermore, in an anti-Thy1.1 model, vitamin D reduced the degree of glomerulosclerosis, suppressing the expression of α-SMA and collagen (13). The foregoing observations suggest that vitamin D may attenuate fibrosis by suppression of myofibroblast activation and proliferation and collagen production. Thus, we hypothesized that vitamin D might inhibit peritoneal fibrosis because myofibroblasts also play a crucial role in peritoneal fibrosis.

Use of $1,25(OH)_2D_3$ is associated with a significant risk of hypercalcemia and hyperphosphatemia. Using it for clinical treatment is therefore not practical. However, 22-oxacalcitriol (OCT) has been reported to be only one one-hundredth as active as $1,25(OH)_2D_3$ in inducing hypercalcemia, although it has a strong biologic activity, including antiproliferative activity and immunosuppressive activity (14).

In the present study, we investigated the potential protective effects of OCT by using an experimental model of peritoneal fibrosis induced by intraperitoneal injection of chlorhexidine gluconate (CG) in which the typical fibrotic features such as marked thickening of the peritoneum, massive collagen accumulation, and myofibroblast proliferation in the submesothelial area develop. We also investigated the possible mechanisms underlying the observed antifibrotic effects of OCT.

METHODS

ANIMALS

The experiments described in this study were conducted using 8-week-old male imprinting control region mice (Japan SLC, Shizuoka, Japan). They were housed in a light- and temperature-controlled pathogen-free room in the Biomedical Research Center, Center for Frontier Life Sciences, Nagasaki University. They had free access to laboratory chow and tap water in standard rodent cages. The experimental protocol was reviewed by the Animal Care and Use Committee of Nagasaki University School and approved by the president of Nagasaki University School (No. 0605220510).

EXPERIMENTAL PROTOCOL

Various groups of mice were compared for the effects of vitamin D treatment on the progression of peritoneal fibrosis according to the experimental protocol, as follows.

Peritoneal fibrosis was induced by intraperitoneal injection of 0.1% CG in 15% ethanol dissolved in saline, as previously described, with some modifications (15,16). Mice received injections of CG into the peritoneal cavity at a volume of 10 mL per kilogram body weight every other day for 3 weeks. The OCT (kindly provided by Chugai Pharmaceutical, Tokyo, Japan), dissolved in phosphate-buffered saline (PBS) containing 0.01% polysorbate 20, was administered by daily subcutaneous injection at 2.0 μg per kilogram body weight (total volume: 200 μL).

To elucidate the "therapeutic" effect of OCT, we performed another experiment in which the mice received CG every other day for 4 weeks. Two weeks after the start of CG injections, these mice were allocated to one of two groups: The mice received either OCT or the vehicle alone for the next 2 weeks. The OCT showed no therapeutic effect (data not shown), and so we focused on the preventive effect of OCT.

Groups of mice received either CG or an equal volume of 15% ethanol in saline as a control. Both groups were further subdivided into two groups each, in which the mice received either OCT or the vehicle alone. Thus, there were a total of four groups: a control group, a CG-only group, an OCT-only group, and a CG+OCT group. Each group included 5 mice. In addition, we used untreated ("normal") mice to elucidate whether VDR is present in normal mouse peritoneum and for histologic examination.

The dose of OCT was selected based on pilot studies that had examined the effects of various OCT doses on

the thickness of the submesothelial area. At 0.5 μg per kilogram body weight, OCT did not reduce peritoneal thickness compared with the thickness observed in non-treated CG mice. Consequently, we selected 2.0 μg per kilogram body weight for the present study. To ensure the injection of the correct dose at the correct site and to avoid pain during injections, all injections were conducted under ether anesthesia.

The mice were humanely killed 21 days after the first CG injection, and the peritoneal tissues were carefully dissected out. To avoid direct damage to the peritoneum by repeated injections, CG was injected into the lower peritoneum, and the upper portion of the parietal peritoneum was used for the subsequent examinations. Immediately after sampling, tissues were fixed with 4% paraformaldehyde in PBS (pH 7.4) and then embedded in paraffin. For histologic examination of peritoneum, 4-μm slices of paraffin-embedded tissues were stained with hematoxylin and eosin.

IMMUNOHISTOCHEMISTRY

Paraffin-embedded tissue sections were stained immunohistochemically using an indirect method. The following antibodies were used for immunohistochemistry: rat anti-chicken VDR antibody diluted 1:25 (GR37: Calbiochem, Darmstadt, Germany); mouse anti-human α-SMA antibody diluted 1:100 (M0851: Dako, Glostrup, Denmark) as a marker for myofibroblasts; rabbit anti–type III collagen antibody diluted 1:400 (LB-1393: LSL, Tokyo, Japan); rabbit anti-human TGF-β antibody diluted 1:100 (sc-146: Santa Cruz Biotechnology, Santa Cruz, CA, USA); rabbit anti-human phosphorylated Smad2/3 antibody diluted 1:50 (sc-11769-R: Santa Cruz Biotechnology); rat anti-mouse F4/80 antibody diluted 1:100 (MCA497: Serotec, Oxford, UK) as a marker of mouse macrophages; and goat anti-mouse anti-monocyte chemoattractant protein 1 (MCP-1) antibody diluted 1:100 (sc-1784: Santa Cruz Biotechnology).

After deparaffinization, the sections were treated with 0.3% H_2O_2 for 20 minutes to inactivate endogenous peroxidase activity. For immunohistochemistry of VDR and phosphorylated Smad2/3, the sections were treated in a microwave oven (MI-77: Azumaya KK, Tokyo, Japan) at 95°C for 15 minutes (VDR) or 5 minutes (phosphorylated Smad2/3) in 10 mmol/L citrate buffer (pH 6.0) before H_2O_2 treatment for antigen retrieval. For immunohistochemistry of α-SMA, type III collagen, TGF-β, F4/80, and MCP-1, the sections were treated with proteinase K (P2308: Sigma, St. Louis, MO, USA) for 15 minutes at 37°C before H_2O_2 treatment for antigen retrieval. The sections were incubated for 30 minutes with a blocking buffer containing 5% normal goat serum, 5% fetal calf serum, 5% bovine serum albumin, and 20% normal swine serum in PBS. The sections were then reacted with the primary antibodies and diluted in the same blocking buffer. For VDR staining, the sections were stained by the avidin–biotin complex technique using a Vectastain Elite ABC kit (Vector Laboratories, Burlingame, CA, USA) after reacting with the first antibody overnight at 4°C. For α-SMA, the sections were reacted for 30 minutes at room temperature with a complex of anti–α-SMA antibody and horseradish peroxidase (HRP)–conjugated rabbit anti-mouse immunoglobulin antibody (P0161: Dako) diluted 1:100 and with HRP-conjugated swine anti-rabbit immunoglobulin antibody diluted 1:50. For type III collagen, after the sections had reacted with anti–type III collagen antibody for 1 hour at room temperature, they were reacted for 30 minutes at room temperature with HRP-conjugated swine anti-rabbit immunoglobulin antibody (P0399: Dako) diluted 1:50. For TGF-β and MCP-1, the sections were stained with the avidin–biotin complex technique using a Vectastain Elite ABC kit after reacting with the first antibody for 60 minutes at room temperature. For phosphorylated Smad2/3, the sections were stained with the avidin–biotin complex technique using a Vectastain Elite ABC kit after reacting with the first antibody for 90 minutes at 4°C. For F4/80, the sections were reacted with HRP-conjugated rabbit anti-rat immunoglobulin antibody (P0450: Dako) and HRP-conjugated swine anti-rabbit immunoglobulin antibody after reacting with anti-F4/80 antibody for 1 hour at room temperature. The reaction products were visualized by treating the sections with H_2O_2 and 3,3′-diaminobenzidine tetrahydrochloride and hydrogen peroxide. Finally, the sections were counterstained with methyl green and mounted. For all specimens, negative controls were prepared using an irrelevant mouse monoclonal antibody, a rat monoclonal antibody, or normal rabbit immunoglobulin G in place of the primary antibody.

Double staining for VDR and α-SMA and for VDR and F4/80 was also performed. After the VDR staining step already described, the sections were washed in PBS to terminate the color reaction and incubated with double-staining enhancer (50–056: Zymed Laboratories, San Francisco, CA, USA). Thereafter, they were reacted with anti–α-SMA or F4/80 antibody and then incubated with HRP-conjugated antibodies as described earlier. A second chromogen, TrueBlue (71-00-68: KPL, Gaithersburg, MD, USA), was then applied, which stained positive cells blue. The tissue sections were not counterstained with methyl green because such counterstaining could interfere with the color from the chromogen.

PREPARATION OF OLIGO DNA AND LABELING

Synthesized double-stranded (ds) DNA was used as a probe. The antisense and sense oligo-DNAs were purchased from Beck's (Tokyo, Japan). The single-stranded (ss) oligo-DNAs (5′-GATCGAGGGGGACTTTCCCTAGC-3′ and 3′-CTAGCTCCCCCTGAAAGGGATCG-5′) were synthesized using the specific consensus sequence for the NF-κB binding site in the promoter region of the immunoglobulin κ light-chain gene (17). For a negative control probe, we used mutated 5′-GATCGAGGAAGACTTTCCCTAGC-3′ and 3′-CTAGCTCCTTCTGAAAGGGATCG-5′. For annealing of complementary ss-oligo-DNAs to ds-oligo-DNAs, the ss-oligo-DNAs were dissolved in 10 mmol/L Tris–HCl buffer (pH 7.4) containing 1 mmol/L EDTA, denatured for 7 minutes at 100°C, and gradually cooled to room temperature. The ds-oligo-DNA was 3′-labeled with digoxigenin using a digoxigenin oligonucleotide tailing kit according to the protocol provided by the supplier (3333566: Roche, Mannheim, Germany).

SOUTHWESTERN HISTOCHEMISTRY

Southwestern histochemistry was performed as previously described (18,19). Deparaffinized tissue sections (4 μm thickness) were washed in PBS, treated in a microwave oven at 95°C for 15 minutes in 10 mmol/L citrate buffer (pH 6.0), and immersed for 60 minutes at room temperature in a pre-incubation buffer containing 5% nonfat milk (198-10605: Wako, Osaka, Japan) dissolved in 50 mmol/L of Tris–HCl (pH 7.4) with 150 mmol/L NaCl and 1 mmol/L EDTA. The sections were then incubated overnight with the probe dissolved in the pre-incubation buffer (2 μg/mL) and washed 4 times (15 minutes each) with 0.075% BRIJ (B4184: Sigma) in PBS. After a brief wash in PBS, the sections were incubated for 60 minutes in a blocking buffer containing 5% bovine serum albumin (102K1265: Sigma), 500 μg/mL normal sheep immunoglobulin G (29H9015: Sigma), 100 μg/mL yeast transfer RNA (R-8759: Sigma), and 100 μg/mL salmon sperm DNA (D-7656: Sigma) in PBS. To visualize the hybridized DNA-oligo probes, the sections were immunohistochemically stained with HRP-conjugated sheep anti-digoxigenin antibody (1207733: Roche) diluted 1:150 in blocking buffer. After 4 washes (15 minutes each) with 0.075% BRIJ in PBS, we visualized the HRP sites in a chromogen solution containing 0.5 mg/mL 3,3′-diaminobenzidine tetrahydrochloride, 0.01% H_2O_2, 0.02% $Ni(NH_4)_2(SO_4)_2$, and 0.025% $CoCl_2$. To evaluate the specificity of the probe for NF-κB, some sections were hybridized with the probe in the presence of an excess amount of non-labeled homologous ds-oligo-DNA. Moreover, some sections were incubated with the mutated probe.

MORPHOMETRIC ANALYSIS

To assess the extent of peritoneal thickening, we used digitized images and image analysis software (Lumina Vision: Mitani Corporation, Tokyo, Japan). We measured the thickness of the submesothelial zone above the abdominal muscle in cross-sections of the abdominal wall. We viewed the image at 200× magnification, randomly selected a field 840 μm wide under the microscope, and then measured the area of the submesothelial layer within the selected field. For each sample, 10 such areas were randomly selected. For each peritoneal sample, the numbers of α-SMA–positive myofibroblasts, TGF-β–expressing cells, phosphorylated Smad2/3–positive cells, F4/80-positive macrophages, MCP-1–expressing cells, and NF-κB–positive cells were counted in 10 fields at 400× magnification. An image analyzer (DAB System: Carl Zeiss, Gottingen, Germany) was used to evaluate cells positive for NF-κB based on the staining density over the level of staining with the sense probe.

BIOCHEMICAL MEASUREMENTS

Serum calcium and phosphate were measured at SRL (Tokyo, Japan).

STATISTICAL ANALYSIS

Data are expressed as means ± standard deviations. Differences between the four groups of mice (control, CG, OCT, and CG+OCT) were examined for statistical significance using repeated-measures analysis of variance (Bonferroni–Dunn test). A value of $p < 0.05$ was considered a statistically significant difference.

RESULTS

EXPRESSION OF VDR IN PERITONEUM

Immunohistochemistry for VDR was performed on mouse peritoneal tissues. In normal mice, a weak but significant signal for VDR was observed in the mesothelial cells [Figure 1(A)]. Expression of VDR was also seen in mesothelial cells in the control and OCT groups (data not shown). Cells positive for VDR were greater in number in the thickened peritoneum in the CG group [Figure 1(B)], but markedly fewer in the CG+OCT group [Figure 1(C)].

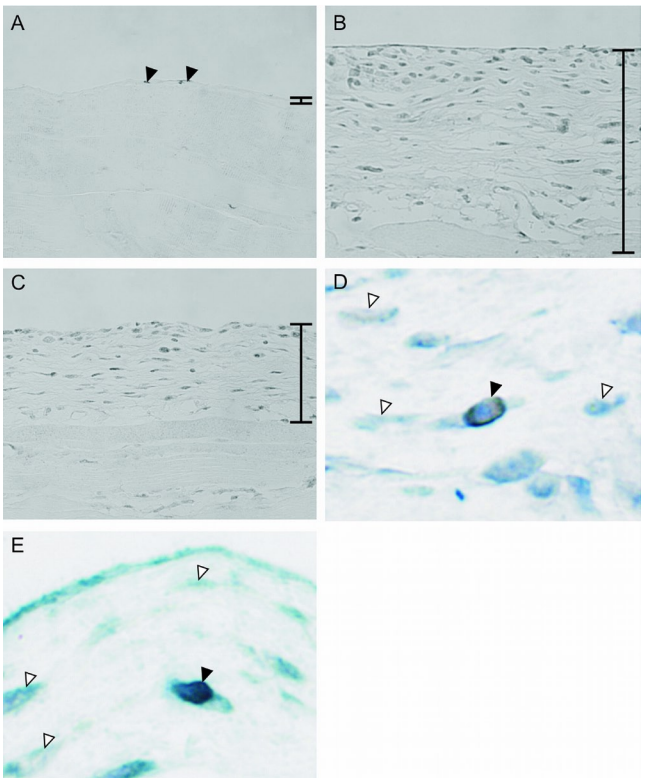

Figure 1 — Immunohistochemistry for the vitamin D receptor (VDR) in peritoneum. (A) In normal mice, VDR was weakly but significantly expressed in mesothelial cells (arrowheads). (B) In the chlorhexidine gluconate (CG) group, the number of cells positive for VDR increased in the thickened submesothelial compact zone. (C) 22-Oxacalcitriol decreased the expression of VDR. Double staining showed that (D) myofibroblasts and (E) macrophages expressed VDR (black arrowhead) in the CG group. White arrowheads indicate negative cells. Bars indicate the thickened peritoneal compact zone. (A–C) Original magnification 200×. (D,E) Original magnification 1000×.

To identify the types of the cells expressing VDR, we performed double staining for VDR with α-SMA, a marker for activated fibroblasts, and with F4/80, a marker for macrophages. The staining revealed that most of the cells expressing VDR were simultaneously positive for α-SMA [Figure 1(D)] and that cells in the peritoneum positive for VDR also expressed F4/80 [Figure 1(E)].

HISTOLOGIC EXAMINATION

Histologic changes were assessed by hematoxylin and eosin staining.

In normal mice, the peritoneal tissue consisted of a peritoneal mesothelial monolayer and an exiguity of connective tissue under the mesothelial layer [Figure 2(A)]. In the control group, the peritoneal tissues were nearly normal, without thickening of the submesothelial zone,

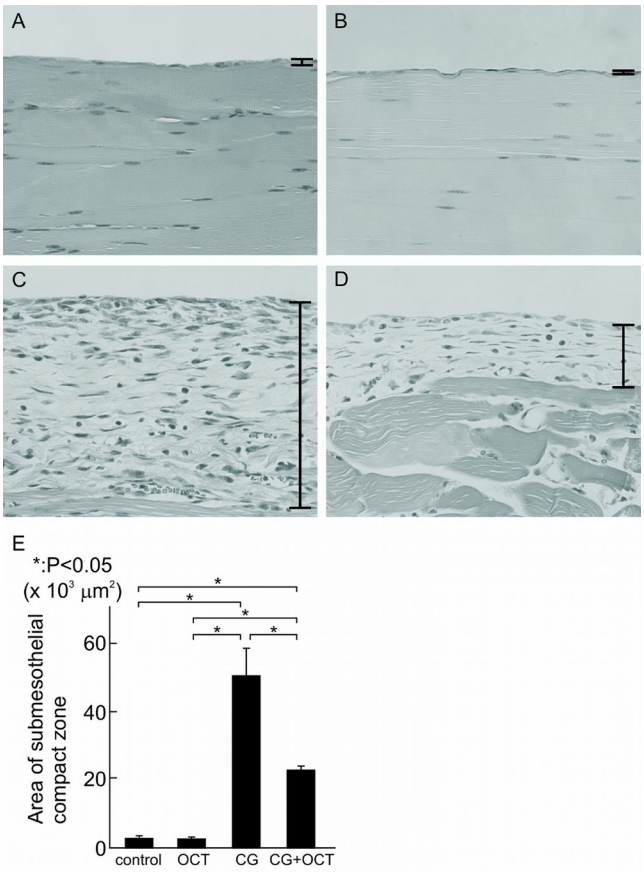

Figure 2 — Hematoxylin and eosin staining of peritoneal tissues. Histogram comparing the thickness of the compact zone between groups, measured over 10 areas 840 μm in width. Values are expressed as mean ± standard deviation (* $p < 0.05$). (A) In normal mice, a monolayer of mesothelial cells covered the entire surface of the peritoneum. (B) In the control group, peritoneal tissues were nearly normal. (C) Peritoneal tissues became thickened and fibrotic in the submesothelial compact zone at 21 days. (D,E) 22-Oxacalcitriol (OCT) significantly prevented the progression of submesothelial thickening. (A–D) Original magnification 200×. CG = chlorhexidine gluconate.

indicating that injection with 15% ethanol did not affect the tissue [Figure 2(B)]. Repeated injections of OCT did not reduce thickening of the peritoneum in the OCT group compared with that in the control group (data not shown).

At day 21, peritoneal samples from the CG group compared with those from the control group showed marked thickening of the submesothelial compact zone and the presence of numerous cells [Figure 2(C)]. However, in the CG+OCT group, the submesothelial thickening was reduced, as was the number of cells [Figure 2(D)]. Quantitative analysis revealed a significant difference between the CG group and the CG+OCT group with respect to the thickness of the compact zone [$p < 0.05$, Figure 2(E)].

EXPRESSION OF α-SMA AND TYPE III COLLAGEN

Figure 3 shows the results of immunohistochemistry for α-SMA, a marker for myofibroblasts, and type III collagen at day 21. In the control group, expression of α-SMA was observed only in vascular smooth muscle cells (data not shown). In the CG group, α-SMA–positive cells were observed in addition to vascular smooth muscle cells, and numerous α-SMA–positive myofibroblasts were identified in the markedly thickened submesothelial compact zone [Figure 3(A)]. Compared with the CG group, the CG+OCT group showed a marked reduction in the number of α-SMA–positive myofibroblasts [Figure 3(B)]. Table 1 summarizes the results of the quantitative analysis of the number of α-SMA–positive cells in the peritoneum in each group.

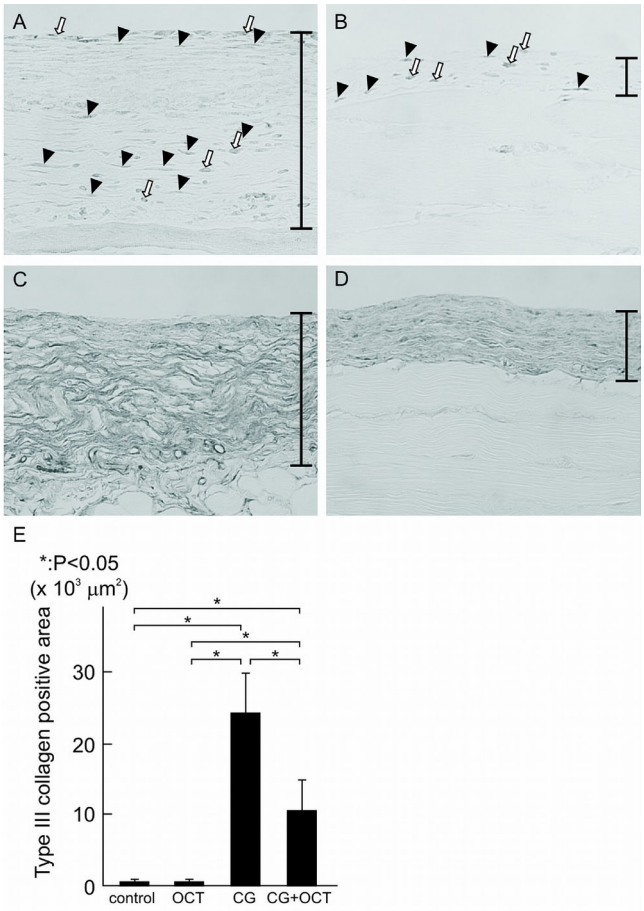

Figure 3 — Immunohistochemistry for α-smooth muscle actin (α-SMA) and type III collagen. Histogram comparing the total surface area positive for type III collagen, measured over 10 areas 840 μm in width. Values are expressed as mean ± standard deviation (* $p < 0.05$). (A) In the chlorhexidine gluconate (CG) group, a number of α-SMA–positive cells were observed in the thickened peritoneal compact zone. Black arrowheads indicate myofibroblasts, and white arrows indicate the other type of cells expressing α-SMA. (B) The number of α-SMA–positive cells were significantly decreased in the CG plus 22-oxacalcitriol (OCT) group. (C) Type III collagen was strongly expressed in the CG group. (D,E) However, expression was lower in the CG+OCT group. (A–D) Original magnification 200×.

We then examined the impact of vitamin D treatment on collagen III expression [as shown in Figure 3(C,D)]. In the CG group, expression of type III collagen was evident in the submesothelial compact zone [Figure 3(C)], but that expression was clearly less in the CG+OCT group [Figure 3(D)]. Semiquantitative analysis showed that expression of type III collagen was higher in the CG group than in the control group, but significantly lower in the CG+OCT group than in the CG group [Figure 3(E)].

EXPRESSION OF TGF-β AND PHOSPHORYLATED SMAD2/3

We used immunohistochemistry to examine the expression of TGF-β, a growth factor that promotes the fibrotic response. In the control and OCT groups alike, very few TGF-β–positive cells were observed in peritoneum (data not shown). The number of TGF-β–positive cells were significantly increased in the thickened peritoneum of the group treated with CG compared with the peritoneum of the control group [Figure 4(A)]. This expression was markedly reduced in the CG+OCT group compared with that in the CG group [Figure 4(B), Table 1].

We also examined phosphorylated Smad2/3, a downstream mediator of TGF-β signaling. A large number of phosphorylated Smad2/3-positive cells were observed in the CG group [Figure 4(C)]. The number of such cells was clearly reduced in the CG+OCT group [Figure 4(D), Table 1].

EXPRESSION OF F4/80, MCP-1, AND ACTIVATED NF-κB

To investigate the effects of OCT on macrophage infiltration, we performed immunostaining for F4/80, a macrophage marker in mice. Cells positive for F4/80 were present in the thickened submesothelial compact zone in the CG group [Figure 5(A)]; in the CG+OCT group, the number of such cells was reduced [Figure 5(B)].

We then examined expression of MCP-1, a potent macrophage chemotactic factor, to investigate the degree to which infiltrating macrophages were decreased in the CG group. We observed that expression of MCP-1 in the submesothelial compact zone was increased in the CG group compared with the control group [Figure 5(C)]. In contrast, expression was reduced in the OCT-treated mice [Figure 5(D)].

We also performed southwestern histochemistry to detect activated NF-κB, a transcription factor

TABLE 1
Immunohistochemistry for α-Smooth Muscle Actin (SMA), Transforming Growth Factor (TGF) β, and Phosphorylated Smad2/3[a]

Molecule	Positive cells in peritoneum (mean ± standard deviation) Control	OCT	CG	CG+OCT
α-SMA	0.4±0.9	0.3±0.6	39.8±8.4[b]	29.7±11.9[b,c]
TGF-β	0.9±0.9	1.0±0.7	80.8±15.5[b]	57.4±16.2[b,c]
Phosphorylated Smad2/3	2.2±1.7	1.6±1.2	72.3±25.4[b]	49.2±12.6[b,c]

OCT = 22-oxacalcitriol; CG = chlorhexidine gluconate.
[a] Cells positive for the various molecules were determined in 10 fields of the submesothelial region selected at random for each mouse and examined at 400× magnification.
[b] $p < 0.05$ vs the control group.
[c] $p < 0.05$ vs the CG group.

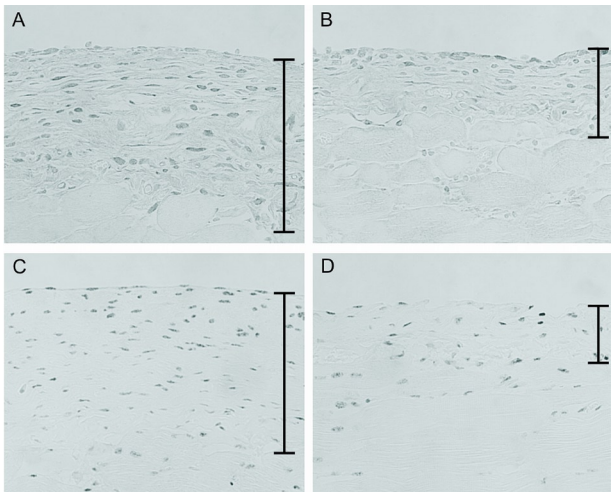

Figure 4 — Immunohistochemistry for transforming growth factor β (TGF-β) and phosphorylated Smad2/3. (A) TGF-β–expressing cells were observed in the peritoneum in the chlorhexidine gluconate (CG) group. (B) However, a significant reduction in TGF-β–expressing cells was observed in the CG plus 22-oxacalcitriol (OCT) group. (C) Many cells positively stained for phosphorylated Smad2/3 were present in the CG group. (D) Treatment with OCT markedly decreased the number of phosphorylated Smad2/3–positive cells. (A–D) Original magnification 200×.

that regulates expression of MCP-1. In the control group, activated NF-κB was not observed in the peritoneum (data not shown). Treatment with CG markedly increased the number of NF-κB–positive cells compared with the number seen in the control group; the types of cells positive for NF-κB were mainly peritoneal mesothelial cells, spindle-shaped fibroblasts, and macrophages [Figure 5(E)]. Treatment of mice with OCT resulted in a significant reduction in NF-κB–positive cells in the peritoneum [Figure 5(F)].

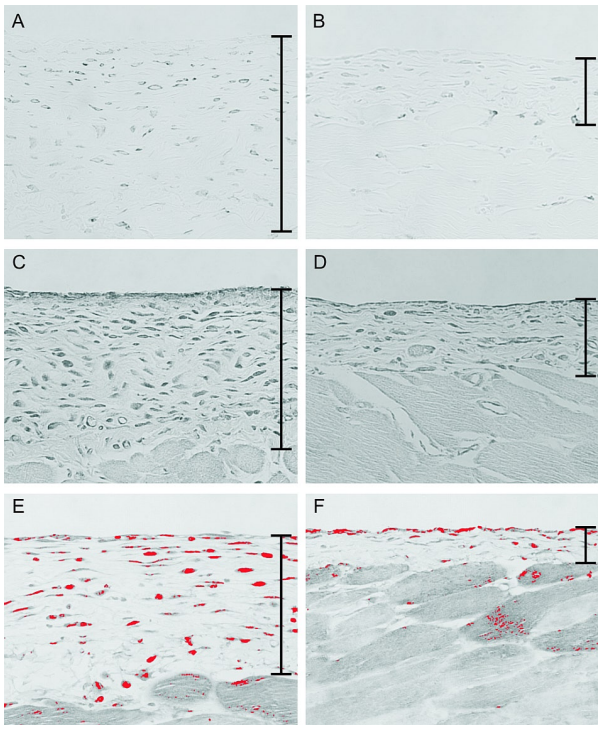

Figure 5 — Immunohistochemistry for F4/80 and monocyte chemoattractant protein-1 (MCP-1) and southwestern histochemistry for activated nuclear factor κB (NF-κB). (A) In the chlorhexidine gluconate (CG) group, a large number of F4/80-positive macrophages were present in the submesothelial zone. (B) Fewer macrophages were observed in the CG plus 22-oxacalcitriol (OCT) group. (C) Cells expressing MCP-1 were present in thickened peritoneal tissues in the CG group. (D) Compared with the CG group, the CG+OCT group showed a reduced number of MCP-1-positive cells. (E,F) The panels of southwestern histochemistry for activated NF-κB were evaluated using an image analyzer. The red color was assigned to positive cells. (E) In the CG group, cells positive for activated NF-κB were detected in the submesothelial compact zone. (F) The number of cells positive for activated NF-κB was significantly lower in the OCT group. (A–F) Original magnification 200×.

Table 2 summarizes the results of the quantitative analysis of the numbers of cells positive for F4/80, MCP-1, and NF-κB in the peritoneum at day 21 for each group.

SERUM CALCIUM AND PHOSPHATE

Because vitamin D plays a major role in calcium homeostasis and bone calcification, and because vitamin D can raise serum calcium and phosphate, we tested whether the study treatments affected calcium and phosphate levels in circulation. Table 3 shows that OCT treatment did not affect serum calcium and phosphate in CG mice. No significant differences in serum calcium and phosphate were observed between the groups.

DISCUSSION

In the present study, we demonstrated that treatment with OCT attenuates the progression of peritoneal thickening and type III collagen deposition induced by injections of CG, concurrent with a reduction in the numbers of myofibroblasts, macrophages, and TGF-β positive cells. These results suggest that vitamin D has potential as a novel therapeutic agent for preventing peritoneal sclerosis.

Although the pathogenesis of peritoneal sclerosis in PD patients remains unclear, many factors are thought to be involved in the development of peritoneal fibrosis. In the present study, we used a mouse model of peritoneal fibrosis induced by intraperitoneal injections of CG. Although the model does not completely mimic human disease, it can be assumed that the development of peritoneal fibrosis follows certain common pathways both in our model and in PD patients. Consistent with that assumption, injection of CG as a nonspecific chemical to induce peritoneal fibrosis produces pathology findings in the peritoneum similar to those seen in PD patients, including increased expression of type III collagen and TGF-β and infiltration by macrophages (15,16). The similarities suggest that the CG model is a useful method for examining the efficacy of various potential therapeutic agents for the prevention of peritoneal fibrosis.

The present study has demonstrated that VDR is expressed in mesothelial cells in the peritoneum. To our knowledge, this is the first report of VDR expression in mouse peritoneal tissue. Our work also shows that VDR expression increases during the development of peritoneal fibrosis induced by CG and is remarkably suppressed by OCT. More recently, Braun *et al.* reported expression of VDR in human peritoneum. Notably, VDR expression

TABLE 2
Immunohistochemistry for F4/80 and Monocyte Chemoattractant Protein 1 (MCP-1), and Southwestern Histochemistry for Activated Nuclear Factor κB (NF-κB)[a]

Molecule	Positive cells in peritoneum (mean ± standard deviation) Control	OCT	CG	CG+OCT
F4/80	0.3±0.7	0.2±0.4	35.1±9.5[b]	15.5±5.7[b,c]
MCP-1	0.2±0.5	0.3±0.5	82.6±23.7[b]	64.3±16.3[b,c]
NF-κB	0.7±0.6	0.5±0.6	22.3±6.8[b]	13.9±6.1[b,c]

OCT = 22-oxacalcitriol; CG = chlorhexidine gluconate.
[a] Cells positive for the various molecules were determined in 10 fields of the submesothelial region selected at random for each mouse and examined at 400× magnification.
[b] $p < 0.05$ vs the control group.
[c] $p < 0.05$ vs the CG group.

TABLE 3
Serum Calcium and Phosphate[a]

	Serum level (mean ± standard deviation) Control	OCT	CG	CG + OCT
Calcium (mg/dL)	12.17±0.40	12.20±0.40	10.92±0.76	11.18±0.51
Phosphate (mg/dL)	12.80±1.45	12.80±1.50	11.64±1.15	11.24±0.42

OCT = 22-oxacalcitriol; CG = chlorhexidine gluconate.
[a] No significant differences were seen between any of the groups.

was more common in the peritoneum of patients with encapsulating peritoneal sclerosis than in the peritoneum of PD patients (20). Because VDR is the specific receptor that mediates the biologic action of vitamin D and its analogs, the presence of VDR in peritoneum supports the pathways discussed herein for inhibition of peritoneal sclerosis.

Recently, Li *et al.* (9) reported that vitamin D is able to block the activation of quiescent fibroblasts and their differentiation into myofibroblasts and to inhibit matrix production by myofibroblasts in the kidney. The suppressive effect of OCT on myofibroblast proliferation is a candidate mechanism for the prevention of peritoneal fibrosis, because in the present study, OCT lowered the number of α-SMA-positive myofibroblasts, which are major collagen-producing cells in the peritoneum.

The pivotal role of TGF-β in the development of peritoneal fibrosis is well known (21). It is central to many fibrogenic processes such as epithelial–mesenchymal transdifferentiation, recruitment of inflammatory cells and fibroblasts, and collagen synthesis (22,23). In the present study, we found that OCT suppressed the number of TGF-β–expressing cells, concurrent with inhibition of mouse peritoneal fibrosis. In addition, expression of phosphorylated Smad2/3, an intracellular mediator of TGF-β signaling in regulation of the fibrotic response, was also diminished by treatment with OCT. Although the mechanism by which OCT suppresses TGF-β remains unknown, it should be noted that crosstalk between the TGF-β and vitamin D signal pathways has been reported. The cooperative action of these molecules can be synergistic or antagonistic in a tissue-specific manner (24,25).

All immortalized cell lines bear the traits of cancer cells, which is a common denominator in the foregoing studies, and various signaling pathways may be activated in animal models of chronic disease. For instance, a model of unilateral ureteral obstruction showed that vitamin D analog suppressed TGF-β1 gene expression (12). In addition, vitamin D reduced TGF-β1 gene expression in a puromycin aminonucleoside nephropathy model (26). Consequently, we suggest that inhibition of TGF-β/Smad signaling may be one of the mechanisms by which OCT exerts an antifibrotic effect in peritoneal fibrosis.

In the present study, we observed a large number of macrophages in the submesothelial zone, and OCT reduced macrophage infiltration as well as peritoneal fibrosis. Because monocytes/macrophages are a known source of several fibrogenic genes, including TGF-β, which is highly correlated with fibrogenic processes, we believe that OCT was able to attenuate peritoneal fibrosis by suppressing macrophage infiltration. The chemokine MCP-1 plays a key role in the recruitment of macrophages, and activation of NF-κB plays an important role in transcriptional control of MCP-1 as described by Tamada *et al.* (27) and references therein. Recent studies have provided evidence for an important role of MCP-1 in the progression of tubulointerstitial fibrosis in the kidney through macrophage recruitment and activation (27,28). Zhang *et al.* (29) reported that a vitamin D analog suppressed high glucose–induced MCP-1 upregulation in mesangial cells by blocking activation of NF-κB. Moreover, in diabetic mice, a vitamin D analog was able to inhibit synthesis and activity of MCP-1 and to ameliorate glomerular injury. Those authors also reported that $1,25(OH)_2D_3$ effectively attenuated MCP-1 induction at both the messenger RNA and transcriptional levels by blocking p65/50 binding to NF-κB sites in the gene promoter. Furthermore, VDR may physically interact with p65 to block p65 binding to DNA, as reported previously for fibroblasts and osteoblasts (30,31). In the present study, we demonstrated that OCT lowered MCP-1 expression and NF-κB activation. Although the underlying mechanism of OCT-induced reduction of infiltrating macrophages in our model is unclear, we hypothesize that OCT exerted an antifibrotic effect by reducing MCP-1 expression via inhibition of NF-κB activation in the peritoneum, subsequently reducing the number of infiltrating macrophages and thereby protecting against peritoneal fibrosis.

It should be noted that the effective dose of OCT for rodents may be different from that for humans, and in the present study, the dose of OCT used for mice is greater than that used for humans. In fact, various doses of OCT have been administered for fibrotic conditions in previous studies. Yang *et al.* (32) showed that addition of $1,25(OH)_2D_3$ to human peritoneal mesothelial cells incubated in medium containing high levels of glucose and lipopolysaccharide reduced the level of TGF-β1 in a dose-dependent manner. In our pilot study, we examined the dose-dependent effects of OCT (0.5 μg per kilogram body weight or 2.0 μg per kilogram body weight) on the thickness of the submesothelial area. As a result, we confirmed the antifibrotic effect of OCT in a dose-dependent manner *in vivo,* which was consistent with the *in vitro* finding of Yang *et al.* Consequently, we selected the dose of 2.0 μg per kilogram body weight for the present study. However, OCT has some adverse effects, such as hypercalcemia and oversuppression of parathyroid hormone. According to previous reports, the incidence of OCT-induced hypercalcemia is high, and the severity of the hypercalcemia is dose-dependent (33). Based on those findings, a higher dose of OCT may show greater reduction of peritoneal fibrosis, but the possibility of hypercalcemia is high. Further studies are therefore needed

to clarify whether OCT can be used to reduce peritoneal fibrosis in PD patients and to examine the suitable dose of OCT for clinical application.

CONCLUSIONS

In the present study, we demonstrated that treatment with OCT suppressed progression of peritoneal thickening and collagen deposition induced by injections of CG. In addition, OCT reduced proliferation of myofibroblasts; infiltration by macrophages; numbers of cells positive for TGF-β, phosphorylated Smad2/3, and MCP-1; and activation of NF-κB. Our results raise the possibility that vitamin D may be a candidate novel therapeutic agent for preventing peritoneal fibrosis. Because vitamin D and its analogs are already used to treat PD patients, a clinical study to evaluate the antifibrotic effect of OCT in peritoneal fibrosis is recommended.

ACKNOWLEDGMENTS

The authors thank Ms. Tomomi Kurashige, Ms. Ryoko Yamamoto, and Ms. Shiho Kondo for invaluable technical assistance. The work reported here was supported by a research grant from the Nonprofit Organization Aimed to Support Community Medicine Research in Nagasaki, Japan.

DISCLOSURES

All authors state that they have no conflicts of interest to declare.

REFERENCES

1. Afthentopoulos IE, Passadakis P, Oreopoulos DG, Bargman J. Sclerosing peritonitis in continuous ambulatory peritoneal dialysis patients: one center's experience and review of the literature. *Adv Ren Replace Ther* 1998; 5:157–67.
2. Gandhi VC, Humayun HM, Ing TS, Daugirdas JT, Jablokow VR, Iwatsuki S, *et al.* Sclerotic thickening of the peritoneal membrane in maintenance peritoneal dialysis patients. *Arch Intern Med* 1980; 140:1201–3.
3. Williams JD, Craig KJ, Topley N, Von Ruhland C, Fallon M, Newman GR, *et al.* on behalf of the Peritoneal Biopsy Study Group. Morphologic changes in the peritoneal membrane of patients with renal disease. *J Am Soc Nephrol* 2002; 13:470–9.
4. Dusso AS, Brown AJ, Slatopolsky E. Vitamin D. *Am J Physiol Renal Physiol* 2005; 289:F8–28.
5. Ebert R, Schütze N, Adamski J, Jakob F. Vitamin D signaling is modulated on multiple levels in health and disease. *Mol Cell Endocrin* 2006; 248:149–59.
6. Dusso AS, Brown AJ. Mechanism of vitamin D action and its regulation. *Am J Kidney Dis* 1998; 32(Suppl 2):S13–24.
7. Rachez C, Freedman LP. Mechanisms of gene regulation by vitamin D_3 receptor: a network of coactivator interactions. *Gene* 2000; 246:9–21.
8. Haussler MR, Whitfield GK, Haussler CA, Hsieh JC, Thompson PD, Selznick SH, *et al.* The nuclear vitamin D receptor: biological and molecular regulatory properties revealed. *J Bone Miner Res* 1998; 13:325–49.
9. Li Y, Spataro BC, Yang J, Dai C, Liu Y. 1,25-Dihydroxyvitamin D inhibits renal interstitial myofibroblast activation by inducing hepatocyte growth factor expression. *Kidney Int* 2005; 68:1500–10.
10. Chen S, Glenn DJ, Ni W, Grigsby CL, Olsen K, Nishimoto M, *et al.* Expression of the vitamin D receptor is increased in the hypertrophic heart. *Hypertension* 2008; 52:1106–12.
11. Biernacka A, Dobaczewski M, Frangogiannis NG. TGF-β signaling in fibrosis. *Growth Factors* 2011; 29:196–202.
12. Tan X, Li Y, Liu Y. Paricalcitol attenuates renal interstitial fibrosis in obstructive nephropathy. *J Am Soc Nephrol* 2006; 17:3382–93.
13. Makibayashi K, Tatematsu M, Hirata M, Fukushima N, Kusano K, Ohashi S, *et al.* A vitamin D analog ameliorates glomerular injury on rat glomerulonephritis. *Am J Pathol* 2001; 158:1733–41.
14. Furuichi T, Kawata S, Asoh Y, Kumaki K, Ohyama Y. Differential time course of induction of 1α,25-dihydroxyvitamin D3–24-hydroxylase mRNA expression in rats by 1α,25-dihydroxyvitamin D3 and its analogs. *Life Sci* 1998; 62:453–9.
15. Nishino T, Miyazaki M, Abe K, Furusu A, Mishima Y, Harada T, *et al.* Antisense oligonucleotides against collagen-binding stress protein HSP47 suppress peritoneal fibrosis in rats. *Kidney Int* 2003; 64:887–96.
16. Yoshio Y, Miyazaki M, Abe K, Nishino T, Furusu A, Mizuta Y, *et al.* TNP-470, an angiogenesis inhibitor, suppresses the progression of peritoneal fibrosis in mouse experimental model. *Kidney Int* 2004; 66:1677–85.
17. Isomoto H, Miyazaki M, Mizuta Y, Takeshima F, Murase K, Inoue K, *et al.* Expression of nuclear factor-κB in *Helicobacter pylori*–infected gastric mucosa detected with southwestern histochemistry. *Scand J Gastroenterol* 2000; 35:247–54.
18. Koji T, Komuta K, Nozawa M, Yamada S, Nakane PK. Localization of cyclic adenosine 3',5'-monophosphate-responsive element (CRE)–binding proteins by southwestern histochemistry. *J Histochem Cytochem* 1994; 42:1399–405.
19. Koji T, Nakane PK. Recent advances in molecular histochemical techniques: *in situ* hybridization and southwestern histochemistry. *J Electron Microsc (Tokyo)* 1996; 45:119–27.
20. Braun N, Fritz P, Biegger D, Kimmel M, Reimold F, Ulmer C, *et al.* Difference in the expression of hormone receptors and fibrotic markers in the human peritoneum—implications for therapeutic targets to prevent encapsulating peritoneal sclerosis. *Perit Dial Int* 2011; 31:291–300.
21. Margetts PJ, Bonniaud P, Liu L, Hoff CM, Holmes CJ,

West–Mays JA, *et al.* Transient overexpression of TGF-β1 induces epithelial mesenchymal transition in the rodent peritoneum. *J Am Soc Nephrol* 2005; 16:425–36.
22. Yang J, Liu Y. Dissection of key events in tubular epithelial to myofibroblast transition and its implications in renal interstitial fibrosis. *Am J Pathol* 2001; 159:1465–75.
23. Bottinger EP, Bitzer M. TGF-beta signaling in renal disease. *J Am Soc Nephrol* 2002; 13:2600–10.
24. Yanagisawa J, Yanagi Y, Masuhiro Y, Suzawa M, Watanabe M, Kashiwagi K, *et al*. Convergence of transforming growth factor-beta and vitamin D signaling pathways on SMAD transcriptional coactivators. *Science* 1999; 283:1317–21.
25. Koli K, Keski–Oja J. Vitamin D3 regulation of transforming growth factor-beta system in epithelial and fibroblastic cells—relationships to plasminogen activation. *J Investig Dermatol Symp Proc* 1996; 1:33–8.
26. Xiao HQ, Shi W, Liu SX, Zhang B, Xu LX, Liang XL, *et al*. Podocyte injury is suppressed by 1,25-dihydroxyvitamin D via modulation of transforming growth factor-β1/bone morphogenetic protein-7 signalling in puromycin aminonucleoside nephropathy rats. *Clin Exp Pharmacol Physiol* 2009; 36:682–9.
27. Tamada S, Nakatani T, Asai T, Tashiro K, Komiya T, Sumi T, *et al*. Inhibition of nuclear factor-κB activation by pyrrolidine dithiocarbamate prevents chronic FK506 nephropathy. *Kidney Int* 2003; 63:306–14.
28. Wada T, Furuichi K, Sakai N, Iwata Y, Yoshimoto K, Shimizu M, *et al*. Up-regulation of monocyte chemoattractant protein-1 in tubulointerstitial lesions of human diabetic nephropathy. *Kidney Int* 2000; 58:1492–9.
29. Zhang Z, Yuan W, Sun L, Szeto FL, Wong KE, Li X, *et al*. 1,25-Dihydroxyvitamin D3 targeting of NF-κB suppresses high glucose-induced MCP-1 expression in mesangial cells. *Kidney Int* 2007; 72:193–201.
30. Sun J, Kong J, Duan Y, Szeto FL, Liao A, Madara JL, *et al*. Increased NF-κB activity in fibroblasts lacking the vitamin D receptor. *Am J Physiol Endocrinol Metab* 2006; 291:E315–22.
31. Lu X, Farmer P, Rubin J, Nanes MS. Integration of the NFκB p65 subunit into the vitamin D receptor transcriptional complex: identification of p65 domains that inhibit 1,25-dihydroxyvitamin D3–stimulated transcription. *J Cell Biochem* 2004; 92:833–48.
32. Yang L, Wang J, Fan Y, Chen S, Wang L, Ma J. Effect of $1,25(OH)_2D_3$ on rat peritoneal mesothelial cells treated with high glucose plus lipopolysaccharide. *Cell Immunol* 2011; 271:173–9.
33. Hirata M, Endo K, Katsumata K, Ichikawa F, Kubodera N, Fukagawa M. A comparison between 1,25-dihydroxy-22-oxavitamin D_3 and 1,25-dihydroxyvitamin D_3 regarding suppression of parathyroid hormone secretion and calcaemic action. *Nephrol Dial Transplant* 2002; 17(Suppl 10):41–5.